Geometric parameters and wear resistance of cam profile of a gas distribution mechanism

Amirkul Irgashev*, *Najmiddin* Mirzaev, *and Behzod* Kurbonov

Tashkent State Technical University, Tashkent, Uzbekistan

Abstract. The paper analyzes the components of the cam profile of a camshaft of an internal combustion engine. The authors developed the method of calculating the width and area of contact, as well as the degree of slippage occurring in the friction pair consisting of a cam and tappet sleeve, resistance to wear of the cam profile, depending on the roughness of the friction surfaces working in the lubricating medium. Studying the wear on the profile of the cam in parts shows that uneven wear occurs along its surface. The values of the parameters affecting the wear process are shown by choosing the wearing environment on the surface of the cam. The trends of changes in the amount of wear in the profile of the cam are presented in the form of a table in the generalized case, and the final conclusions are reached based on the calculation results.

1 Introduction

The profile of the cam is integrally connected with the timely opening and closing of the intake and exhaust cam, ensuring the sequence of the processes between the piston and the cylinder as a result of the interaction with the push sleeve. It is important to perform the processes carried out in the internal combustion engine at the required level in the operating conditions, to ensure the required curvature of the characteristic areas of the cam profile within the permissible bending limit.This requirement can be characterized by three cases depending on the wear of the cam profile. The first and third of them allow the piston to move smoothly between the bottom and top dead centers of the cylinder, and the second ensures the smooth movement of the piston between the dead centers of the cylinder, which ensures the generation of a stable torque depending on the load on the crankshaft and its transmission to the transmission aggregate.

2 Materials and research methods

The contact between Cam of the camshaft and pusher bushing has a significant effect to wear on the cam profile. In the internal combustion engine (Figure 1), the problem of rolling friction is solved in this friction pair.For this purpose, the shaft profile is machined to create a slope of 1.5º relative to the axis of the distribution shaft, and as a result of the formation of a spherical surface with a volume radius of 42 mm on the end of the sleeve in connection

* Corresponding author: irgashevamirkul@mail.ru

with the sleeve, the length of the pusher sleeve is 2. 2 mm point contact is formed on the shoulder (in the case where the friction pair is not affected by the normal load), sliding caused the change of friction to rolling friction and the reduction of the frictional force in this friction pair.

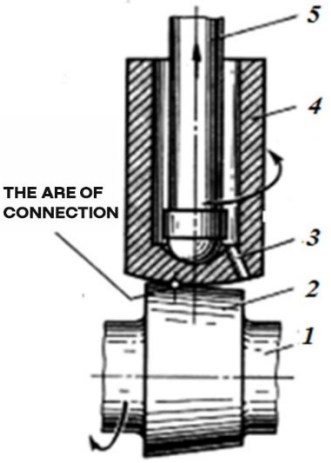

Fig. 1. Connection diagram between the camshaft sleeve and the pusher: 1 – gas distribution shaft; 2 – cam; 3 – lubrication hole; 4 – pusher sleeve; 5 – pusher.

3 Research results and discussion

The force generated by the elastic deformation acting along the axis of the spring is transmitted through the pusher to the pusher sleeve. As a result, an elastic (resilient) contact area is formed around the contact point of the friction pair.

The profile of the intake and exhaust camshafts of the engine consists of 6 characteristic states.

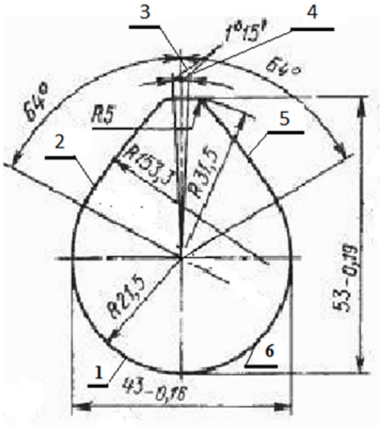

Fig. 2. Scheme of placement of the characteristic parts of the input cam.

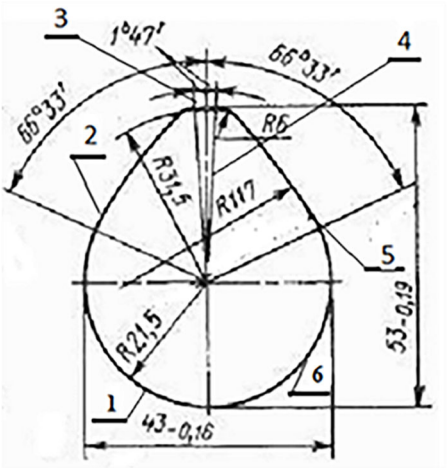

Fig. 3. Scheme of the placement of the characteristic parts of the output cam.

In cases 1 and 6, the profile of cam has a constant radius of curvature, the center of which corresponds to the center of rotation of the bushing, in which the friction pair consisting of the bushing and the pusher sleeve receives a constant, minimum load, therefore, the bending of this part of the bushing profile is the same as that of the rest of the bushing profile. will have the smallest value relative to the parts.

Cases 2 and 5 of the profile of cam are characterized by constant radius of curvature, the center of which is located outside the center of rotation of the cam. In this case [1], due to the vertical deformation of the valve spring, a variable load is applied to each connection point of the cam profile [18]. At the starting point of this part of the cam profile, the load has a minimum value, and at the end point it has a maximum value. Cam profile states 4 and 5 have a radius passing through the center of the cam, where the process (at the end of the compression stroke and the exhaust stroke) occurs at the top dead center of the piston [11].

In general, the length of the state of the cam,

$$l_i = \frac{2\alpha_i \cdot r_i}{360}, mm \quad (1)$$

Where, α_i - is the angle of coverage of the cam position; r_i - is the radius of curvature of the cam position. The dependence of the cylinder profile and the given radius of the thrust sleeve on the angle of coverage of the cylinder position, the radius of curvature and the radius of curvature of the thrust are presented in Tables 1 and 2.

Table 1. The given radius of curvature of the characteristic states of the cam profile.

The sequential order of the situation of cam	**The coverage angle of cam position, grad**	**The curvature radius of the cam, mm**	**The curvature radius of the thrust sleeve, mm**	**The specified radius of curvature of Cam profile and pusher sleeve, mm**
1	116.00	21.5	42.0	14.20
2	62.75	153.3	42.0	32.97
3	1.25	31.5	42.0	18.00
4	1.25	31.5	42.0	18.00
5	62.75	153.3	42.0	32.97
6	116.00	21.5	42.0	14.20

1 - the results of the calculations presented in the tables were determined based on the following preliminary data:

1 – in the table: Angle of coverage of the position of cam, degree: 116.00; 62.75; 1.2.;

Radius of curvature of the cam position, mm: 21.5; 153.3; 31.5.

When analyzing the lengths of the intake and exhaust cam profiles, it was found that the difference in length of the intake cam profile is 21.880 mm longer than the length of the exhaust cam profile.

This difference was 16.20% of the length of the inlet and 19.34% of the length of the outlet. According to the data presented in table 3, the difference in the length of the inlet and outlet profiles is not the same. In cases 1, 2, 4, and 6, the profile of the inlet valve is greater than the length of the outlet valve [12], showing that the length of the inlet valve profile is 0.02% of the length of the case 1. 6, and 7.92% of the length of the case 2, 5.

Table 2. Calculation of the total length of the cam profile and its analysis.

Position of cam	Intake cam			Exhaust cam			The difference in the lengths of the cam profiles, mm
	The coverage angle of the cam, grad	Radius of the cam	Length of the cam profile, mm	The coverage angle of the cam, grad	Radius of the cam	Length of the cam profile, mm	
1	116.00	21.5	13.856	113.45	21.5	13.550	0.306
2	62.75	153.3	53.440	65.00	117.0	42.752	10.688
3	1.25	31.50	0.218	1.55	56.18	0.272	-0.054
4	1.25	31.50	0.218	1.55	56.18	0.272	-0.054
5	62.75	153.3	53.440	65.00	117.0	42.752	10.688
6	116.00	21.5	13.856	113.45	21.5	13.550	0.306
The total length of the cam profile, mm			135.028	The total length of the cam profile, mm		113.148	21.880

The high efficiency of the exhaust cam can be explained by the high pressure of the used gas generated by the combustion process in the cylinder, and it should also be considered that the opening angle of the exhaust valve is 24% higher than that of the exhaust cam.

3.1 Calculation of the contact width and contact area of the pusher and cam

In the resulting analytical expression, the normal load acting on the friction pair consisting of the cam profile and the pusher was replaced by the stiffness of the valve spring and its multiplication by its vertical deformation. In cases where the elastic deformation of the connection between the sleeve profile and the holder sleeve is not taken into account, the connection occurred at the point, and in practice, the elastic deformation is equal to each other along the axis of the cam and in sections perpendicular to it, an expression for calculating the width of the connection was derived.

Table 3. Dependence of the contact width and contact area of the cam and pusher on the spring deforming force.

Position of cam	Intake cam			Exhaust cam		
	Spring deformer power, N	Cam and pusher pair connection width, mm	Cam and pusher pair connection area, mm^2	Spring deformer power, N	Cam and pusher pair connection width, mm	Cam and pusher pair connection area, mm^2
1	264	0.508	0.262	264	0.508	0.262
2	308	0.709	0.508	308	0.694	0.486
	352	0.741	0.554	352	0.726	0.532
	396	0.771	0.600	396	0.755	0.575
	440	0.799	0.643	440	0.782	0.618
	484	0.825	0.685	484	0.807	0.657
	528	0.849	0.727	528	0.831	0.696
	572	0.872	0.766	572	0.854	0.734
	616	0.894	0.805	616	0.875	0.771
	660	0.915	0.842	660	0.896	0.806
3	704	0.764	0.587	704	0.764	0.587
4	704	0.764	0.587	704	0.764	0.587
	660	0.915	0.842	660	0.896	0.806
	616	0.894	0.805	616	0.875	0.771
	572	0.872	0.766	572	0.854	0.734
	528	0.849	0.727	528	0.831	0.696
	484	0.825	0.685	484	0.807	0.657
	440	0.799	0.643	440	0.782	0.618
	396	0.771	0.600	396	0.755	0.575
	352	0.741	0.554	352	0.726	0.532
5	308	0.709	0.508	308	0.694	0.486
6	264	0.508	0.262	264	0.508	0.262

Dependence of the connection width of the cam and the pusher sleeve and the connection surface, the spring deforming force and the specified radius of the friction surfaces are presented in table 3. According to it, the stiffness of the spring material, the compression deformation of the spring with the cam [7], the increase of the given radius of the friction pair formed by the cam and pusher, and the increase of the connection width.

The width of the elastic deformation of the surface of the cup is given by the following expression:

$$B_{k,c} = 2.1 \cdot \left(\frac{\sqrt{z_{n\cdot} \cdot h \cdot \rho_{kel}} \cdot (1-\mu^2)}{\sqrt{E_{kel}}} \right)^{0.67}, \quad (2)$$

Where, z_n - is the stiffness of the valve spring, N/mm; h – vertical deformation of the valve spring, mm; μ - Poisson's coefficient; E_{kel} - modulus of elasticity, MPa.

Also, the friction between the cam profile and the pusher sleeve occurs according to the scheme presented in Figure 1, and the pair involved in the connection of the friction surfaces can occur in a fixed position.

In this case, it is assumed that the connection between the cam and the pusher sleeve consists of a point, and in practice [6], the probability of the connection of these surfaces being deformed during the friction process is high considering that it has a value that is too

low to be taken into account, the contact spot formed by the contact of the friction surfaces can be assumed to be circular.

In it, the following expression was derived to calculate the contact area between the circular sleeve and the pusher sleeve,

$$F_{k,cm} = 4.39 \cdot \left(\frac{\sqrt{z_{n\cdot} \cdot h \cdot \rho_{kel}} \cdot (1-\mu^2)}{\sqrt{E_{kel}}} \right)^{1.34} . \quad (3)$$

Taking this expression into account the roughness of the spring material, the vertical deformation of the valve spring [3], the specified radius of curvature of the spherical part of the cam profile and the pusher sleeve, the calculated values of the contact area of the inlet and outlet cam profile consisting of characteristic parts are presented in table 4.

The rate of wear of the cams depends on the degree of relative sliding that occurs between the pusher surfaces. Their values are generally the following expression for calculating the value of each constituent part of the cam profile:

for the input cam profile,

$$\delta_{ki} = \frac{L_{ki} - L_{ci}}{L_{ki}} ; \quad (4)$$

for exhaust cam profile,

$$\delta_{ci} = \frac{L_{ci} - L_{ci}}{L_{ci}} . \quad (5)$$

Table 4 shows the distribution of the slip created due to the difference in the length of the profile parts of the cam by the parts of these cams.

3.2 Dependence of the wear resistance of the camshaft profile on the roughness of the friction surfaces

If there are no abrasive particles in the environment in which the friction pair works, causing it to be contaminated, the grinding process occurs only with the presence of burrs that participate in the friction process [8].

Table 4. The relative slip that occurs in the friction pair of the cam profile and the pusher sleeve depends on the radius of curvature of the bushing and dependence on compressive strength.

Cam part indicators			Valve spring		The distribution of slip by cam conditions
Position	**Angle, grad.**	**Radius of the arc, mm**	**Deformation in height, mm**	**Squeezer power, N**	
1	116	21.5	46	264	0.0111
2	62.75º	153.3	45	308	0.1211
	62.75º	153.3	44	352	0.1211
	62.75º	153.3	43	396	0.1211
	62.75º	153.3	42	440	0.1211
	62.75º	153.3	41	484	0.1211
	62.75º	153.3	40	528	0.1211
	62.75º	153.3	39	572	0.1211
	62.75º	153.3	38	616	0.1211
	62.75º	153.3	37	660	0.1211
3	1.25º	31.5	36	704	0.2360
4	1.25º	31.5	36	704	0.2360

5	62.75º	153.3	37	660	0.1285
	62.75º	153.3	39	616	0.1285
	62.75º	153.3	40	572	0.1285
	62.75º	153.3	41	528	0.1285
	62.75º	153.3	42	484	0.1285
	62.75º	153.3	43	440	0.1285
	62.75º	153.3	44	396	0.1285
	62.75º	153.3	45	352	0.1285
	62.75º	153.3	46	308	0.1285
6	116	21.5	48	264	0.113

The following expression is proposed to calculate the total deflection rate that occurs between the grooves of the friction surfaces consisting of the cam profile and the pusher sleeve:

$$\gamma_{k,c} = \frac{F_{k,c} \cdot s_{k,c} \cdot M_{k,c} \cdot n_{k,c} \cdot \eta_{k,c}}{F_{k,cm} \cdot n_{pk,c}}, \quad (6)$$

Where, $F_{k,c}$ – the cross-sectional area of the metal volume, immersed in the friction surface of the cams, deformed by a single bumpy bump, modeled in a spherical shape; $s_{k,c}$ - sliding path of the cam profile; $M_{k,c}$ -the number of bumpy protrusions located in the width of the connection of the cam profile; $n_{k,c}$ - the frequency of rotations of the input (output) cam; $\eta_{k,c}$ - the possibility of re-deformation of the surface of the input (output) cam; $F_{k,cm}$ - the area formed by the connection of the input (output) cam with the pusher sleeve; $n_{p(k,c)}$ - the number of cycles leading to failure of the deformed surface of the input (output) cam.

The following analytical relation was derived to calculate the volume of the deformed friction surface with all the burrs of the intake (exhaust) cam profile at the junction of the pusher sleeve:

$$v_{k,c} = F_{k,c,m} \cdot s_{k,c} \cdot M_{k,c} \quad (7)$$

The area of the cross-section of the deformed metal volume formed as a result of the penetration of a single ridge-bulge into the friction surface of the profile of the intake (exhaust) cam is calculated by the following expression.

$$F_{k,c} = \frac{H_{k,c} \cdot (6 \cdot a_{k,c} + 8 \cdot b_{k,c})}{15} = \frac{0.65 \cdot P_{k,c}^2 \cdot \theta}{B_{k,c}^2 \cdot c \cdot \sigma_{tk,c}}, \quad (8)$$

Where, $P_{k,c}$ – the normal compressive force resulting from the vertical deformation of the spring of the intake and exhaust cam; θ – elasticity constant; $a_{k,c}$ and $b_{k,c}$ - ball cement vaters of the cam's bulge, which is modeled in a spherical form, formed by the immersion of the ball into the friction surface; c - coefficient of deformation; $\sigma_{tk,c}$ - the flow limit of the material of the cam; $H_{k,c}$ - the hardness of the cam material.

The sliding path of the cam profile depends on the degree of sliding between the friction surfaces and the length of the cam profile states, it is expressed as follows:

$$s_{k,c} = \delta_{ki} \cdot l_i \quad (9)$$

Where, δ_{ki} - the level of sliding in cases *1, 2 , ... , i* of the profile of the cam, respectively; $l_1; l_2; ...; l_i$ - the length of the ash profile in *1, 2 ,…, i* - states, respectively.

The number of burrs located in the width of the connection of the cam [5], the width of the connection of the input (exhaust) cam, the number of burrs in the connection increases with the increase of the yield point of the materials of the friction pairs, the increase of the pressure in the friction pair and the radius of curvature increases the number of burrs involved in the bending process leads to a decrease,

$$M_{k,c} = \frac{B_{k,c} \cdot c \cdot \sigma_{t(k,c)} \cdot E_{kel}}{14.275 \cdot p_{k,c}^2 \cdot \rho_{kel}}. \quad (10)$$

Where, $B_{k,c}$ - the connection width of the cam; $p_{k,c}$ - pressure between the cam and the pusher sleeve,

$$p_{k,c} = \frac{P_{k,c}}{F_{k,c}}, \quad (11)$$

Where, $F_{k,c}$ - the area of the connection of the cam and the pusher sleeve.

The volume of metal deformed by bumps on the surface of the cam in contact with the pusher sleeve,

$$v_{k,c} = \frac{0.04553 \cdot P_{k,c}^2 \cdot \theta \cdot E_{kel} \cdot \delta_{ki} \cdot l_i}{B_{k,c} p_{k,c}^2 \cdot \rho_{kel}}. \quad (12)$$

The possibility of re-deformation of the deformed surface of the cylinder head profile is obtained by replacing the normal compressive force $P_{k,c}$, formed by the vertical deformation of the spring of the intake and exhaust valves $p_{k,c}$, to the pressure between the cam profile and the pusher sleeve:

$$\eta_{k,c} = \frac{0.0389 \cdot p_{k.c}^2 \cdot \rho_{kel}}{B_{k,c} \cdot c \cdot \sigma_{t(k,c)} \cdot E_{kel}}. \quad (13)$$

It was determined that the number of loads that cause deformation of the friction surfaces of the cam profile depends on the roughness of the fracture surfaces involved in the friction process, their relative elongation coefficient ψ and the friction fatigue index of the fractures t involved in the friction process [14], which is expressed as follows.

$$n_{pk,c} = \psi_{k,c}^t \quad (14)$$

The value of determined $F_{k,c}$ from the expression (29); value of $s_{k,c}$ from the expression (10) ; value of $M_{k,c}$ from the expression (11); value of $n_{k,c}$; $\eta_{k,c}$ from the expression (14); the value of $F_{k,cm}$ from the expression (4) and substituting the value of $n_{pk,c}$ from the expression (15) to (7) and after some simplifications, the following analytical relation is obtained for calculating the bending speed of the ash profile:

$$\gamma_k = \frac{6,376 \cdot P_k^2 \cdot \theta \cdot (1+\delta_{ki}) \cdot n_k}{B_k^3 \cdot \sigma_{t(k)} c \cdot n_{pk}} \text{ mm/ h.} \quad (15)$$

5 - the following preliminary data were used to calculate the bending speed of the profile of the input and output cams presented in the table: elasticity constant θ=4.23·10^{-6}*MPa*$^{-1}$; the yield point of the material of the cam $\sigma_{t(k)} = 1300 MPa$; the frequency of

rotations of the cam $n_k = 20s^{-1}$; the number of loadings that cause deformation of the deformed volume of the friction surfaces of the cam profile $n_{pк} = 24$; the total length of the cam profile $L_k = 135.028mm$; coefficient of deformation $c = 3$.

Table 5. The results of calculation of the rate of wear without the presence of abrasive particles on the friction surface of the input cam profile.

Parts of cam profile	Valve spring deformer power, N	connection width of cam and pusher, mm	Current length of cam profile parts, mm	Current deflection angle of cam profile parts, °	Wear rate of the cam profile mm/h
1	264	0.508	13.856	116.00	0.000891
2	308	0.709	53.442	6.97	0.001719
	352	0.741	53.442	13.94	0.002111
	396	0.771	53.442	20.91	0.002309
	440	0.799	53.442	27.88	0.002453
	484	0.825	53.442	34.85	0.002695
	528	0.849	53.442	41.82	0.002943
	572	0.872	53.442	48.79	0.003188
	616	0.894	53.442	55.76	0.003431
	660	0.915	53.442	62.73	0.003674
3	704	0.764	0.218	1.25	0.007916
4	704	0.764	0.218	1.25	0.007916
5	660	0.915	53.442	62.73	0.003674
	616	0.894	53.442	55.76	0.003431
	572	0.872	53.442	48.79	0.003188
	528	0.849	53.442	41.82	0.002943
	484	0.825	53.442	34.85	0.002695
	440	0.799	53.442	27.88	0.002453
	396	0.771	53.442	20.91	0.002309
	352	0.741	53.442	13.94	0.002111
	308	0.709	53.442	6.97	0.001719
6	264	0.508	13.856	116.00	0.000891

Based on the angle of coverage of the parts of the cam profile, the radius of curvature and the radius of curvature of the pusher sleeve [16], the given radius of the cam profile and the sleeve pair was determined, which allows to calculate the width of the connection of the sleeve profile and the sleeve and the contact surface.

4 Conclusion

When analyzing the lengths of the cam profiles, it was found that the length of the intake manifold profile is 21,880 mm longer than the length of the exhaust cam profile, this difference is 16.20% of the intake cam length and 19.34% of the exhaust cam length.

It was determined that due to the difference in the length of the parts of the cam profile, different values of sliding are formed in the parts of the cam profile: the largest value of this difference is 10.688 mm in parts 2 and 5 of the cam profile, 0.306 mm in parts 1 and 6, and 0.054 mm in parts 3-4 corresponded to.

It was determined that the contact width and contact area of the friction pair consisting of the cam profile and the pusher sleeve depend on the stiffness of the valve spring, the vertical

deformation of the spring, and the given radius of the pair of the cam profile and the pusher sleeve.

The speed of friction of the friction surfaces of the cam profile increases according to the degree of sliding between the rubbing parts, linearly with respect to the frequency of rotations of the sleeve, and parabolic with respect to the normal force generated by the deformation of the valve springs, the first and third levels of width of the sleeve material increase the friction resistance of the sleeve profile will come.

References

1. A. Yu. Zamyatin, V. Yu. Zamyatin, Friction and wear **1** 394-397 (2021)
2. K. V. Journeymen, Friction and wear **(2)3** 18-21 (2000)
3. A. Tukhtakuziyev, Sh. U. Ishmuradov, R. B. Abdumajidov, IOP Conf. Ser.: Earth Environ. Sci. **868** 012058 (2021)
4. D. G. Tigetov, Yu. A. Goritsky, Friction and lubrication in machines and mechanisms **3** 4-13 (2010)
5. Q. Q. Mirzayev, A. Irgashev, Journal of Friction and Wear **35(5)** 439-442 (2014)
6. V. E. Starzhinsky, Y. L. Solimterman, E. I. Tesker, A. M. Goman, S. A. Osipenko, Friction and wear **5**, 465-482 (2008)
7. S. T. Yunuskhodjaev, Journal of Physics: Conference Series **2176**, 012045 (2022)
8. U. Ikramov, A. Irgashev, K. Kh. Makhkamov, Friction and wear **24(6)**, 620-625 (2003)
9. V. V. Grib, Expert Solutions, 448 (2014)
10. SH. U. Ishmuradov, R. B. Abdumajidov, IOP Conf. Ser.: Earth Environ. Sci. **1076** 012039 (2022)
11. B. A. Irgashev, Allerton Press **36(5)**, 441-447 (2015)
12. Kh. Ishmuratov, R. K. Hamroev, B. B. Kurbonov, N. N. Mirzaev, Journal of Physics: Conference Series **2176(1)**, 012096 (2022)
13. Sh. A. Sultanova, J. E. Safarov, A. B. Usenov, D. Muminova, Journal of Physics: Conference Series **2176**, 012007 (2022)
14. D. G. Tigetov, MPEI Bulletin **6**, 119-128 (2008)
15. Sh. U. Zulpanov, D. I. Samandarov, G. T. Dadayev, S. A. Sultonova, J. E. Safarov, IOP Conf. Series: Earth and Environmental Science **1076**, 012059 (2022)
16. Sh. A. Sultanova, A. A. Artikov, Z. A. Masharipova, Abhijit Tarawade, J. E. Safarov, IOP Conf. Series: Earth and Environmental Science **868**, 012045 (2021)
17. H. K. Ishmuratov, B. A. Irgashev, Journal of Friction and Wear **41(1)**, 85-90 (2020)
18. N. N. Mirzayev, B. B. Qurbonov, R. K. Hamroyev, Technical science and innovation **4(06)**, 198-204 (2020)